

SELF-CONSISTENT MODELLING OF THE
POLAR THERMOSPHERE AND IONOSPHERE
TO MAGNETOSPHERIC CONVECTION AND PRECIPITATION
(Invited Review)

David Rees, Tim Fuller-Rowell,
Department of Physics and Astronomy,
University College London,
Gower Street, London WC1E 6BT, UK

Shaun Quegan
Marconi Space and Defense Systems, Chelmsford UK
Roy Moffett
Applied Maths. Dept., Sheffield University, Sheffield, UK

It has recently been demonstrated that the dramatic effects of plasma precipitation and convection on the composition and dynamics of the polar thermosphere and ionosphere include a number of strong interactive, or feed-back, processes. To aid the evaluation of these feed-back processes, a joint three dimensional time-dependent global model of the earth's thermosphere and ionosphere has been developed in a collaboration between University College London and Sheffield University. This model includes self-consistent coupling between the thermosphere and the ionosphere in the polar regions. Some of the major features in the polar ionosphere, which the initial simulations indicate are due to the strong coupling of ions and neutrals in the presence of strong electric fields and energetic electron precipitation will be reviewed. The model is also able to simulate seasonal and UT variations in the polar thermosphere and ionospheric regions which are due to the variations of solar photoionization in specific geomagnetic regions such as the cusp and polar cap.

INTRODUCTION

Two three-dimensional time-dependent models of the global thermosphere have been developed as diagnostic tools to aid the evaluation of empirical thermospheric data^{1, 2}. These models have included descriptions of the major energy and momentum inputs to the thermosphere, such as solar UV and EUV heating, and the geomagnetic polar inputs caused by the combined effects of energetic particle precipitation and the magnetospheric convective electric field imprinted on the polar regions^{3, 4, 5}.

The descriptions of the geomagnetic inputs have been somewhat improved by iterative ionospheric/thermospheric modelling^{6, 7}. It has been possible to model the polar ionosphere as influenced by magnetospheric precipitation and solar illumination, and as modified by ionospheric convection and thermospheric winds which have themselves been driven by ion drag resulting from the combination of enhanced plasma densities and strong convection. This ionosphere, plus the particle precipitation energy and convection electric field has then been used to generate the

resulting patterns of thermospheric winds, and the consequent changes of thermospheric density, composition and temperature.

The precipitation and convection models used in these initial attempts were, however, very idealized, and it was only possible to iterate between the ionospheric and thermospheric models by a laborious data base exchange once per 24 hours UT. Fully time-dependent, and UT-dependent computations could not be carried out by this method, although the results represented, for the polar ionosphere and thermosphere, a major advance over the use of the global 'Chiu' ionosphere⁸, which has no contribution which can be recognized as due to the influence of the magnetospheric processes. The compositional effects of the geomagnetic input were not passed back to the ionospheric model, rather the MSIS empirical model was used to predict thermospheric composition under representative solar, seasonal and geomagnetic conditions.

More complex precipitation patterns⁹ and convection patterns¹⁰, using a one-dimensional solution to the ionospheric effects of the precipitation, based on Roble and Rees (1977), have been used in an interim attempt to study the response of the polar thermosphere to severe geomagnetic disturbances. These attempts have been a useful means of representing the enhancement of ionospheric conductivity, ion drag and frictional heating both in the simulation of average geomagnetic input conditions^{12, 13} and for storm-time simulations^{14, 15}. Plasma transport effects due to convection and winds are, however, crucial at F-region altitudes. Additionally, the feedback of induced changes of thermospheric composition, which changes rapidly and locally during intense geomagnetic disturbances, is an important omission in previous ionospheric modelling studies.

To overcome these limitations, a strategy has been developed which permits the combination of 3-D T-D global thermospheric model and a polar/auroral ionosphere model to be run with the frequent interchange of the inter-dependent parameters. Firstly, however, the description of the geophysical processes which occur within the ionosphere have had to be updated, compared with the descriptions used in previous work^{6, 7}.

The computational and data base strategy, permitting the frequent interchange of essential parameters, and the detailed physical content of the new ionospheric code will be described in detail in a series of papers now in preparation, however, it is appropriate to cover the major elements which have been changed since the prior work (i.e.^{6, 7, 12}).

DESCRIPTION OF THE JOINT MODEL

I. THE IONOSPHERIC CODE

The polar ionospheric code developed at Sheffield University for simulating structures of the polar ionosphere, the plasmasphere, and the causes of complex phenomena such as the mid-latitude trough, has been described in a series of papers^{6, 7, 16}. The earlier model dealt primarily with the problems of the upper F region, and its extension either into the plasmasphere, or into the high-altitude polar ionosphere. The light atomic ions, essentially O⁺, He⁺, and H⁺, were thus the most important components of the ionospheric code.

In dealing with the lower parts of the ionosphere, below about 200 km, many aspects of the original code have had to be modified. Molecular ions, which have much more rapid recombination rates than atomic ions, tend to dominate over the atomic ions in the increased presence of molecular nitrogen and molecular oxygen. As a result, residence times are thus much shorter, so that transport effects, particularly due to horizontal transport, become less important. However, strong vertical movements of ionization, resulting from fast horizontal convection, and also from rapid horizontal and vertical wind motions, must be considered.

Next, the strategy of data interchange between two vastly different styles of models has to be optimised:

The thermosphere model exists on a regular global grid, using spherical coordinates in the horizontal dimension, and with pressure coordinates in the vertical dimension. The global grid rotates with the earth.

The ionosphere model exists as a series of one-dimensional, time-dependent solutions to the conditions within a hypothetical flux tube. The contents of these flux tubes are influenced by precipitation, solar photoionization, and recombination and charge exchange processes (etc), as the flux tubes are convected through regions where the geophysical conditions vary greatly.

A typical flux tube in the polar regions is convected throughout the dayside and nightside parts of the polar cap and auroral oval, experiencing highly variable solar photo-ionization, particle precipitation and convection velocity. The flux tube will also be convected through regions where the temperature and composition of the thermosphere, in addition to the wind velocity, will be highly variable. For convenience, the convection paths followed by individual flux tubes are used as the fundamental grid of the ionospheric model.

Even when the only time-dependence in the model is that induced by the UT-dependent location of the geomagnetic polar regions with respect to solar illumination, each flux tube has to be followed for many hours. As the flux tube convects throughout the high latitude regions, the solution will eventually become convergent and stable to the input conditions, which can vary over extreme ranges as flux tubes convect into and out of sunlight, or regions of strong convection and/or precipitation.

A sequence of points thus have to be followed along each convection path, so that at any specific Universal Time, there is a reasonably uniform distribution of populated flux tubes along each of the convection paths which are used in the computations.

II. THE THERMOSPHERIC CODE

The UCL three dimensional time-dependent global thermospheric model has been described in detail in a number of recent papers¹²⁻¹⁵. The only significant change created in the interactive and self-consistent modelling approach is that, in the high latitude regions, the earlier computation of the ionosphere from either the CHIU global model (applicable to quiet geomagnetic conditions only), or by the PIONS ionospheric model¹⁴⁻¹⁵, is now replaced by the ionospheric computations described conceptually above. For the gain of realism, the additional computation involved in this procedure uses only marginally greater computer resources than the previous ionospheric computation from the CHIU model, or from implementing the PIONS routine.

PRESENT STATUS

The present status of this work is that early diagnostic tests of the joint code have been run, to test the numerical method and code, and to examine the sensitivity of the resulting ionosphere to the range of geomagnetic and solar/seasonal conditions.

Several of the early interesting results from these tests will be discussed, with their significance for the future adaption of the joint code to the routine computation of self-consistent global models of the thermosphere and ionosphere.

SIMULATIONS WITH STEADY-STATE GEOMAGNETIC INPUTS

Some major results of the work of Quegan et al⁶, and Fuller-Rowell et al⁷ will be summarized. The 'Sheffield' model, used a geometry of co-incident geographic and geomagnetic poles (UT-independent), and were carried out for the northern polar region at winter solstice. Separately, the polar ionosphere and the global thermosphere models were run to stability, and the relevant data sets were interchanged (ionospheric density distribution transferred to the thermosphere model, and thermospheric winds etc transferred to the ionospheric model). This data set interchange was iterated once (after 24 hours). The resulting thermospheric and ionospheric data were convergent after this single iteration.

The polar ionosphere and thermosphere wind system resulting from these early computations⁶ are shown at 320 km altitude in Figure 1. For comparison, Figure 2 shows the polar ionosphere and the thermospheric wind system produced by the CHIU ionosphere model.

In the polar ionosphere, the auroral enhancement of plasma density is very pronounced, and a 'hole' has appeared in the polar cap as a result of plasma stagnation with this particular polar electric field. Around the boundaries of the auroral oval, features similar to the trough associated with the plasmapause have appeared^{6, 16}.

In comparison with empirical data, two major factors must be considered. Firstly, although the values used to describe the magnetospheric precipitation are by no means extreme, individual flux tubes are exposed to this precipitation for many hours within both the dusk and the dawn parts of the auroral oval. Secondly, there is no feed-back into the thermospheric composition in this early simulation, so that one important consequence of intense enhancement of ion-neutral momentum coupling, namely the strong enhancement of molecular nitrogen density in thermospheric regions which are strongly heated by frictional or particle heating, does not occur due to use of the MSIS global model.

The very long exposure to persistent (if moderate) particle fluxes, and the lack of thermospheric compositional response, generates ionospheric plasma densities within the auroral oval which are probably higher than would really occur. Naturally time-dependent ionospheric convection, where individual flux tubes are carried into and out of regions of auroral precipitation, and the enhancement of nitrogen density in regions of strong thermospheric heating, causing a major increase in the effective ionospheric recombination rate, are likely to suppress the high modelled auroral electron density values.

Features such as the ionospheric 'polar hole', which have been observed in satellite data, are due, in the model simulations, to stagnation regions, where plasma remains caught up in polar cap regions on the night-side where there is no precipitation and where there is no solar photo-ionization.

In reality, such conditions may rarely occur, and Killeen et al¹⁷ have recently shown that regions of major polar cap plasma depletions may be the signature of intense ion-neutral coupling in regions of very fast anti-sunward ion flow.

TIME-DEPENDENT JOINT SIMULATIONS

The structure of both thermospheric and ionospheric parts of the model has been created so that there is an easy interchange of data sets between the two models. At present, one or other model is being run independently, in virtually the same mode used in the original study⁶. The exception is that thermospheric composition can be passed between the models, and a sequence of simulations are in progress to examine the effects of closing feedback loops such as the geomagnetic effects on thermospheric composition.

The structure of the models is organized in such a way that, with a minimum time constant of 15 minutes, the geomagnetic inputs to the polar ionosphere and thermosphere can be varied. Ultimately, this will allow the realistic simulation of strongly time-dependent events. At this stage, the major limitation to exploitation of the joint ionospheric/thermospheric model will then be the limited availability of truly global data sets describing the geomagnetic input to the polar ionosphere and thermosphere.

SIMULATIONS OF THE POLAR IONOSPHERE

The first simulations using the new ionospheric code have used, as part of the input, the thermospheric wind system derived from 3D TD model simulations for approximately equivalent seasonal, solar activity and geomagnetic activity. Simulations have been carried out for the summer and winter solstices and for the equinox. As a result of these simulations, it is possible to see the effects of variable solar photo-ionization, and of seasonally-variable thermospheric composition in the polar regions.

Although the simulations have been carried out for a full range of Universal Times, the results will only be displayed at a single UT for each of the four simulations to be described. Two of the simulations use the 'A2' polar convection field (Figure 3¹⁰) to describe the northern hemisphere polar convection when the IMF Y component is negative. The last simulation, for northern winter solstice, uses the 'B2' polar convection field (Figure 4), corresponding to a condition when the IMF Y component is positive. The convection paths, followed by individual flux tubes, responding to these convection patterns, as seen from the sun, are shown in Figures 5 and 6 respectively.

For all of these simulations, a background thermospheric wind model, which is approximately that corresponding to the situation for which we are now generating the ionospheric model, has been used. The neutral gas composition and temperature for these initial simulations have been taken from MSIS¹⁷, preparatory to running the full interactive model.

A. THE POLAR IONOSPHERE AT WINTER SOLSTICE:

Northern Hemisphere, A2 convection, IMF BY negative

Figures 7 and 8 show the polar plasma densities at 18 UT at altitudes of 160 and 320 km respectively. At each altitude, the auroral enhancement of plasma density is pronounced, as is the mid-latitude peak of plasma density in the early afternoon hours on co-rotating flux tubes below the latitude of the auroral oval.

B. THE POLAR IONOSPHERE AT SUMMER SOLSTICE:

Northern Hemisphere, A2 convection field (IMF BY negative)

In Figures 9 and 10, the ionospheric structure for the same UT is shown for the summer solstice (N. Hemi.). In this simulation, the peak electron densities in the auroral oval are considerably lower than in the winter simulation. This is due to the greater amount of molecular nitrogen, at the equivalent altitude and pressure level, in the upper thermosphere at the summer solstice, causing an increase in the effective ionospheric recombination rate, which more than offsets the increased solar photo-ionization in this summer period. As a result, the electron densities fall to about 50% of the peak values obtained in the winter solstice simulation.

In Figure 11, the corresponding plasma density distribution from the Chiu model is shown for the northern summer polar region. The peak number densities are not too different, however, the entire distribution has changed, so that the effects of plasma precipitation are most marked, while the mid-latitude densities of the theoretical model are significantly below those of the Chiu model.

DISCUSSION

IONOSPHERIC STRUCTURES IN THE POLAR REGIONS

The dominating structure seen in the polar plasma densities is the enhancement of electron density in the vicinity of the auroral oval, at all altitudes, and during summer and winter solstice conditions. The plasma density enhancements are due to the prolonged exposure of individual flux tubes to magnetospheric precipitation as these flux tubes convect sunward within both the dusk and the dawn parts of the auroral oval. Although the precipitating fluxes are modest, the duration of exposure is prolonged (several hours). The peak plasma densities appear to be rather higher than occur in the real world, and we anticipate that this is due to the prolonged exposure of individual flux tubes to magnetospheric precipitation, with inadequate feed-back due to compositional change.

In the real world, under quiet and moderately disturbed geomagnetic conditions, the flux tubes may experience much more variable convection and precipitation, which reduce the average ion generation. Also, thermospheric feed-back mechanisms, not yet allowed to operate fully (compositional changes), may act to deplete plasma densities on flux tubes which spend long periods within the auroral oval.

SEASONAL VARIATIONS

The seasonal variations of plasma density are in the sense which has been reported by Foster¹⁹ from observations with the Millstone Hill Incoherent Scatter Radar. That is, the dayside electron densities are higher in winter than in summer, and the peak auroral oval plasma densities are likewise higher in winter than in summer. In the present simulations, this is due to the higher concentration of molecular species in the MSIS summer polar thermosphere. Since this is also a feature of the UCL 3-D T-D model^{13, 15, 20}, this seasonal anomaly in polar plasma density will, undoubtedly, also be a feature of the fully coupled ionosphere and thermosphere model.

VARIATIONS WITH THE Y COMPONENT OF THE IMF

The major variations which are induced by changing the polar convection field are only seen at the higher altitudes, where recombination is slower, and where the transport of plasma causes a strong modification of the plasma distribution. Figures 8 and 10 (BY negative) illustrate the pattern created when the highest anti-sunward ion flow regions is the dusk side of the polar cap.

A tongue of enhanced plasma density reaches back across the polar cap on the dusk side when BY is negative. This is very reminiscent of the structures described by Weber et al²¹. They have reported anti-sunward convecting patches of enhanced ionospheric plasma density and related features of polar cap airglow features.

When the region of highest anti-sunward flow moves to the dawn side of the polar cap (BY positive), the plume of enhanced plasma density follows this change in the polar convection, and creates a quite asymmetrical plasma distribution compared with Figures 8 and 10.

In the joint modelling studies which have been carried out so far, the wind structures (3-D T-D model) and the thermospheric composition and temperature structures (MSIS for comparable conditions) which have been imposed as input conditions to the ionospheric model are moderately close to the conditions we would expect to develop. This does not, however, allow the full feed-back processes to develop, particularly in thermospheric temperature and composition. The major effects which would be anticipated as a result of closing the feed-back loop are associated with the enhancement of recombination coefficients in regions where there is strong ion-neutral coupling and frictional heating, or where there is strong particle heating. These fully-coupled simulations will be carried out in the near future, and it will then be possible to examine the conclusions mentioned earlier relating to the regions of strong depletion of polar cap plasma densities.

A significant problem which has to be solved in the near future is how to introduce a better method of preventing the plasma densities within the auroral oval from reaching unrealistically large values. Possibly, the explanation lies in the feed-back coupling of enhancement of molecular neutral and thus ionic species in those regions where there is intense heating for long periods, as plasma is forced to remain on convection paths which remain for long periods in regions such as the dusk auroral oval. Another possibility is that the temporal variations of precipitation and convection ensure that, in the real world and under slightly to moderately disturbed conditions, specific flux tubes are continuously moving into and out of regions of significant precipitation. In this way, the enhancement of plasma density would be rather more modest.

Accounting for this latter mechanism in a theoretical model is not a trivial process, but represents one of the outstanding goals of simulating in a realistic way the structure of the polar ionosphere under a range of realistic seasonal, solar and geomagnetic conditions, where the major feed-back mechanisms between the ionosphere and polar thermosphere are taken into account.

Acknowledgements

The development of the joint ionospheric and thermospheric model has reflected discussions with a large number of scientists currently active in Solar-Terrestrial Physics. We are particularly indebted to Israel Perla and Robert Gordon for assistance with the development and running of the model code at UCL. There have also been a number of valuable discussions with David Evans, David Winningham, Jim Heppner, Nelson Maynard, Tim Killeen and Larry Brace, which have greatly helped the evolution of the fabric of the joint model, and the description of the particle and plasma convection environment of the polar regions. The UK Science and Engineering Research Council supported the computing facilities, and provided research grants to University College London. Many of the model simulations which provided the background to this study were carried out using the CRAY 1-S of the University of London Computer Centre, and the UCL node of the UK STARKLINK facility.

REFERENCES

1. FULLER-ROWELL T. J. and REES D. (1980). A three-dimensional time-dependent global model of the thermosphere *J. Atmos. Sci.* **37**, 2545-2567.
2. ROBLE R. G., DICKINSON, R. E., and RIDLEY E. C. (1982). Global Circulation and Temperature Structure of the Thermosphere with High-latitude Plasma Convection *J. Geophys. Res.* **87**, 1599-1614.
3. HINTEREGGER H. E. (1981). Representation of solar EUV fluxes for aeronomical applications. *Adv. Space Res.* **1**, 39-52.
4. KNUDSEN W. C., BANKS P. M., WINNINGHAM J. D. and KLUMPAR D. M. (1977). Numerical model of the convecting F2 ionosphere at high latitudes. *J. Geophys. Res.* **82**, 4784-4792.
5. HEPPNER J. P. (1977). Empirical models of high latitude electric fields. *J. Geophys. Res.* **82**, 1115-1125.
6. QUEGAN S., BAILEY G. J., MOFFETT R. J., HEELIS R. A., FULLER-ROWELL T. J., REES, D., and SPIRO R. W. (1982). A Theoretical Study of the distribution of Ionization in the High Latitude Ionosphere and the Plasmasphere: first results on the Mid-latitude Trough and Light-ion trough. *J. Atmos. Terr. Phys.* **44**, 619-640.
7. FULLER-ROWELL T. J., REES D., QUEGAN S., BAILEY G. J., and MOFFETT R. J. (1984). The effect of realistic conductivities on the high-latitude neutral thermospheric circulation. *Planet. Space Sci.* **32**, 469-480.
8. CHIU Y. T. (1975). An improved phenomenological model of ionospheric density. *J. Atmos. Terr. Phys.* **37**, 1563-1570.
9. SPIRO R. W., REIFF P. F. and MAHER L. J. (1982). Precipitating electron energy flux and auroral zone conductances—an empirical model. *J. Geophys. Res.* **87**, 8215-8227.
10. HEPPNER J. P. and MAYNARD N. M. (1983). Paper presented at Chapman Conference at Irvington Virginia. March, 1983.
11. ROBLE R. G. and REES M. H. (1977). Time dependent studies of the aurora: Effects of particle precipitation on the dynamic morphology of ionospheric and atmospheric properties. *Planet. Space Sci.* **25**, 991.
12. REES D., FULLER-ROWELL T. J., GORDON R., KILLEEN T. L., HAYS P. B., WHARTON L. E. and SPENCER N. W. (1983). A Comparison of Wind Observations of the Upper Thermosphere from the Dynamics Explorer Satellite with the Predictions of a Global Time-dependent Model. *Planet. Space Sci.* **31**, 1299-1314.
13. REES D. (1985). Theoretical Thermosphere Models. Paper presented at COSPAR, Graz (1984). To be published *Adv. Space Res.*
14. REES D., FULLER-ROWELL T. J., SMITH M. F., GORDON R., KILLEEN T. L., HAYS P. B., SPENCER N. W., WHARTON L., MAYNARD N. C. (1985). The Westward Thermospheric Jet-Stream of the Evening Auroral Oval. Accepted by *Planet. Space Sci.*
15. REES D., SMITH M. F. and GORDON R. (1984). The Generation of Vertical Thermospheric Winds and Gravty Waves at Auroral Latitudes - II. Theory and Numerical Modelling of Vertical Winds. *Planet. Space Sci.* **32**, 685-705.
16. MOFFETT R. J. and QUEGAN S. (1983). The Mid-Latitude Trough in the Electron Concentration of the Ionospheric F-Layer: a review of observations and modelling. *J. Atmos. Terr. Phys.* **45**, 315-343.

17. KILLEEN T. L., HAYS P. B. CARIGNAN G. R., HEELIS R. A., HANSON W. B., SPENCER N. W. and BRACE L. H. (1984). Ion-Neutral Coupling in the High-Latitude F Region: Evaluation of Ion Heating Terms From Dynamics Explorer 2. *J. Geophys. Res.* **89**, 7495-7508.
18. HEDIN A. E., REBER, C. A., NEWTON G. P., SPENCER N. W., BRINTON H. C., MAYR H. G., and POTTER W. E. (1977). A global thermospheric model based on mass spectrometer and incoherent scatter data. MSIS 2. Composition. *J. Geophys. Res.* **82**, 2148-2156.
19. FOSTER J. C. (1984). Ionospheric Signatures of Magnetospheric Convection. *J. Geophys. Res.* **89**, 855-865.
20. HEDIN A. E., REES D. and FULLER-ROWELL T. J. (1985). In preparation.
21. WEBER E. J., BUCHAU J., MOORE J. G., SHARBER J. R., LIVINGSTON R. C., WINNINGHAM J. D. and REINISCH B. W. (1984). F Layer Ionization Patches in the Polar Cap. *J. Geophys. Res.* **89**, 1683-1694.

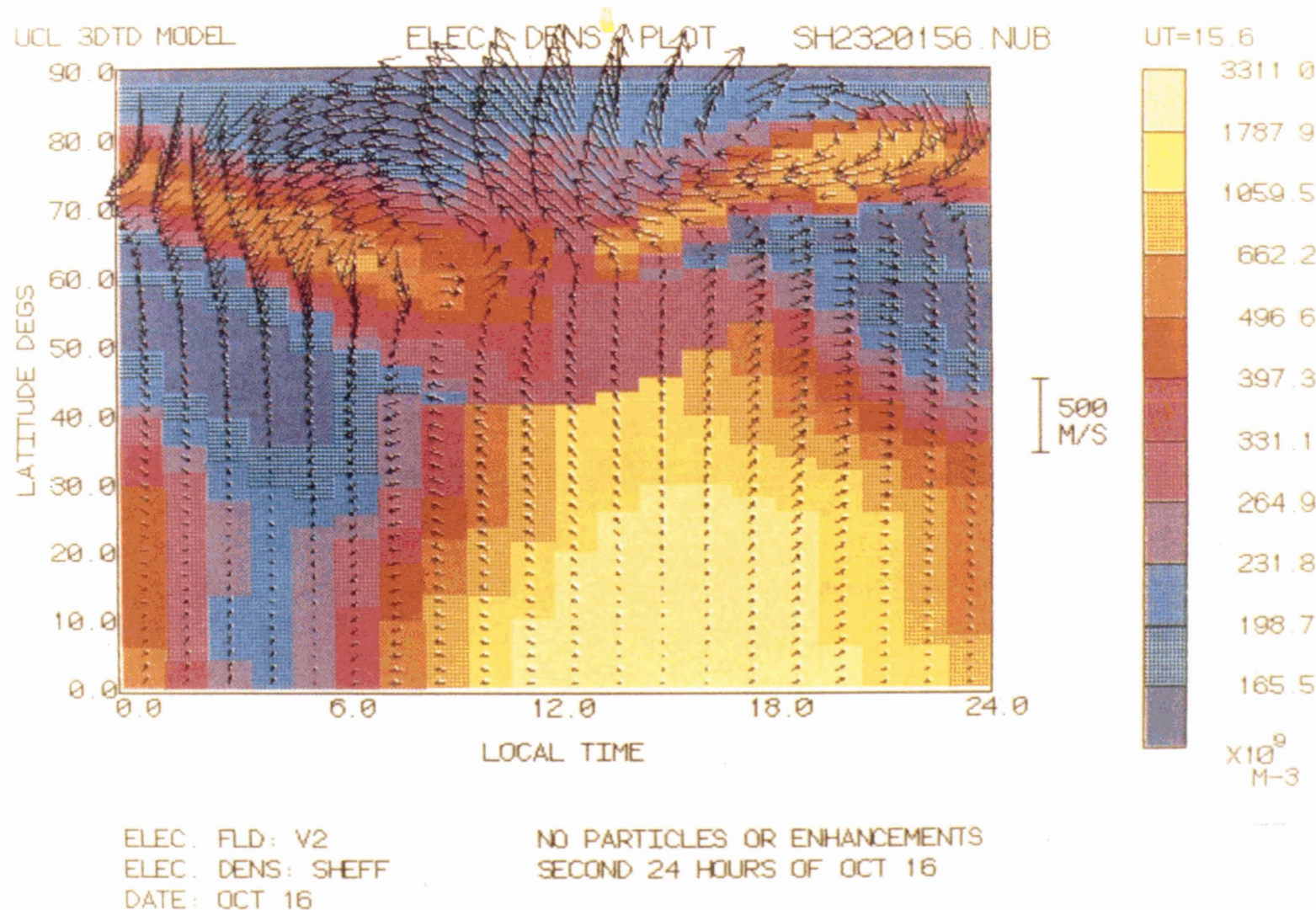


Figure 1. Thermospheric wind system at 320 km produced by the 'Sheffield' polar electron density model, in combination with the Heppner model B2 polar electric field. The polar presentation is in geographic coordinates, and the contours of the electron density distribution are also shown. The enhancement of electron density around the dusk and dawn parts of the auroral oval is distinct.

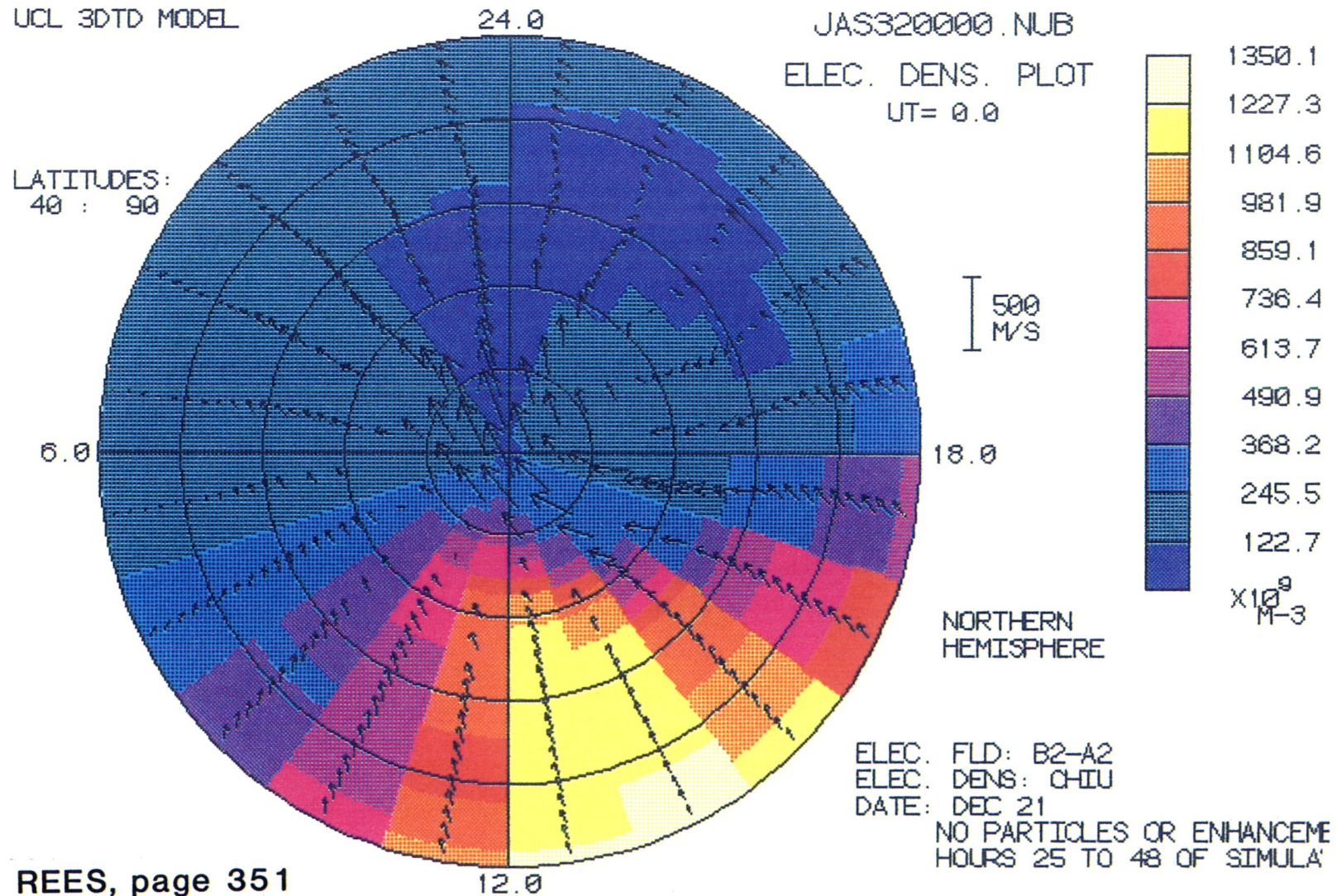
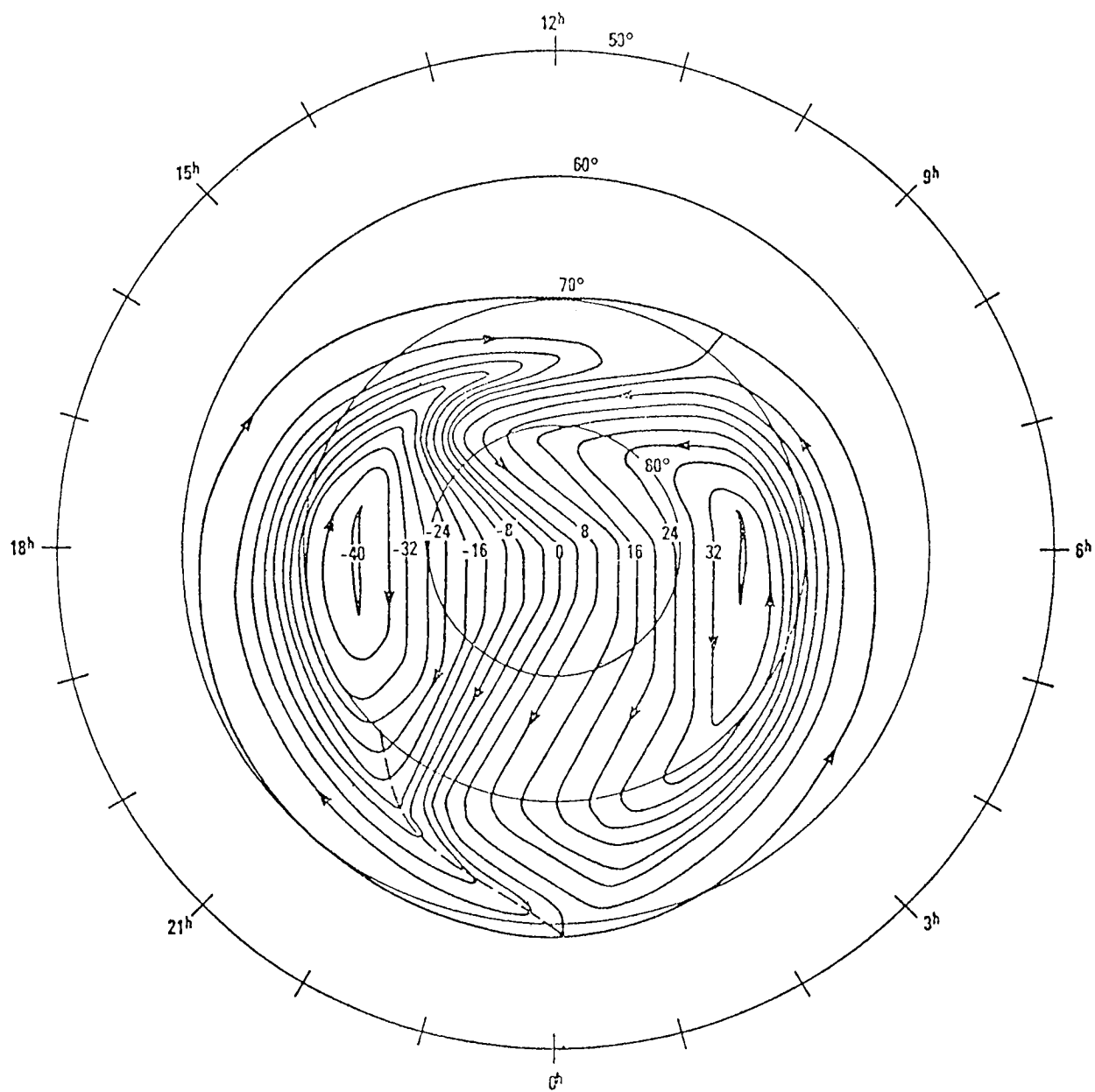
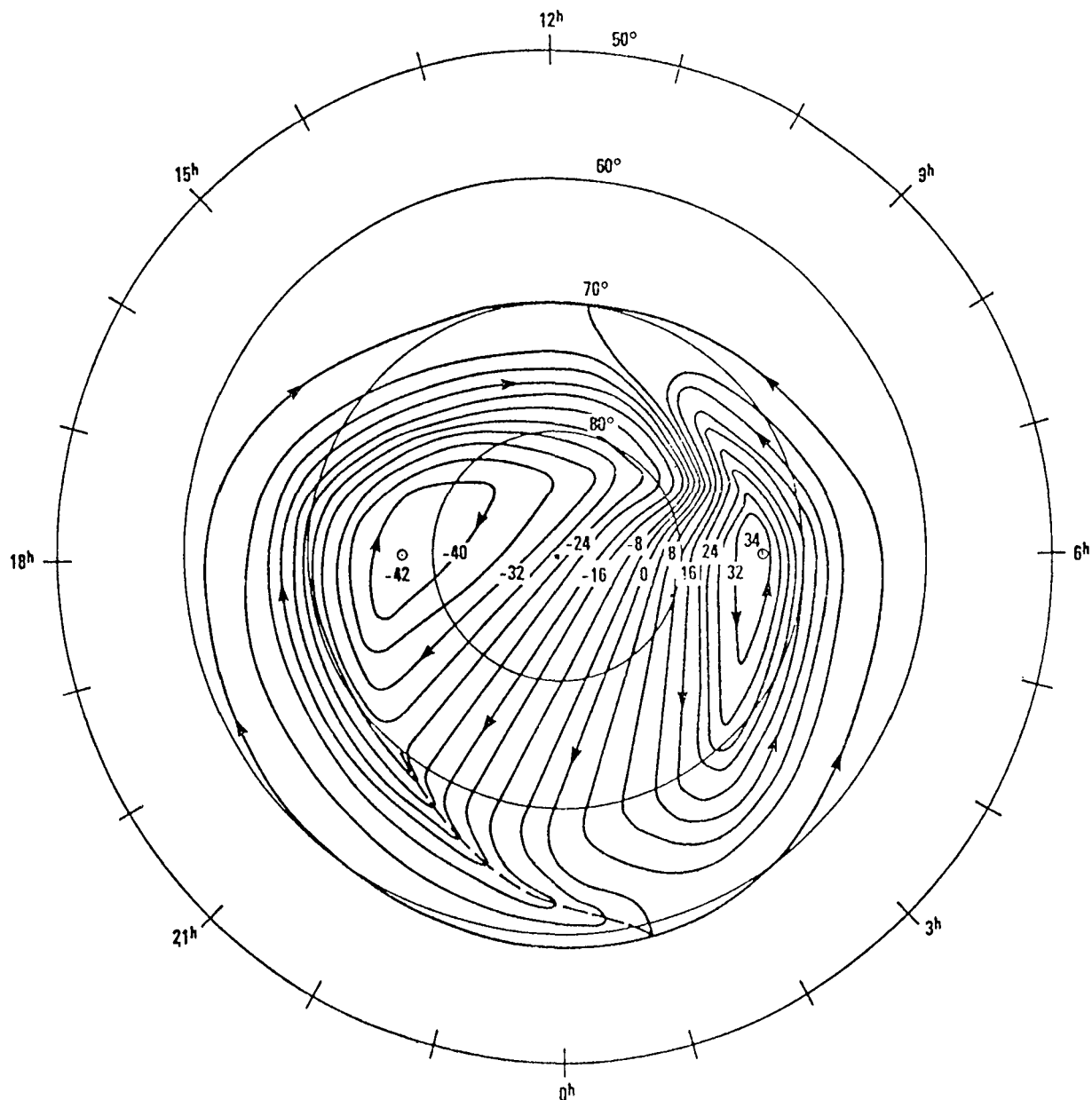


Figure 2. Thermospheric wind system at 320 km produced by the 'Chiu' global ionospheric model, with the same polar electric field as used to produce Figure 1. The much lower electron densities can be seen from the scalar background values. The winds in the auroral oval are significantly lower, approximately half the value of those produced by the 'Sheffield' ionosphere.



MODEL A-2

Figure 3. The A2 model of the polar electric field, from Heppner and Maynard 1983. This field is applied to the northern hemisphere when the IMF BY component is negative, and to the southern polar region when the IMF BY component is positive. It applied to moderately disturbed geomagnetic conditions $3 < kp < 4$ (approx.).



MODEL B-2

Figure 4. The B2 model of the polar electric field, from Heppner and Maynard 1983. This field is complementary to the A2 field, i.e. is applied to the northern hemisphere when the IMF BY component is positive.

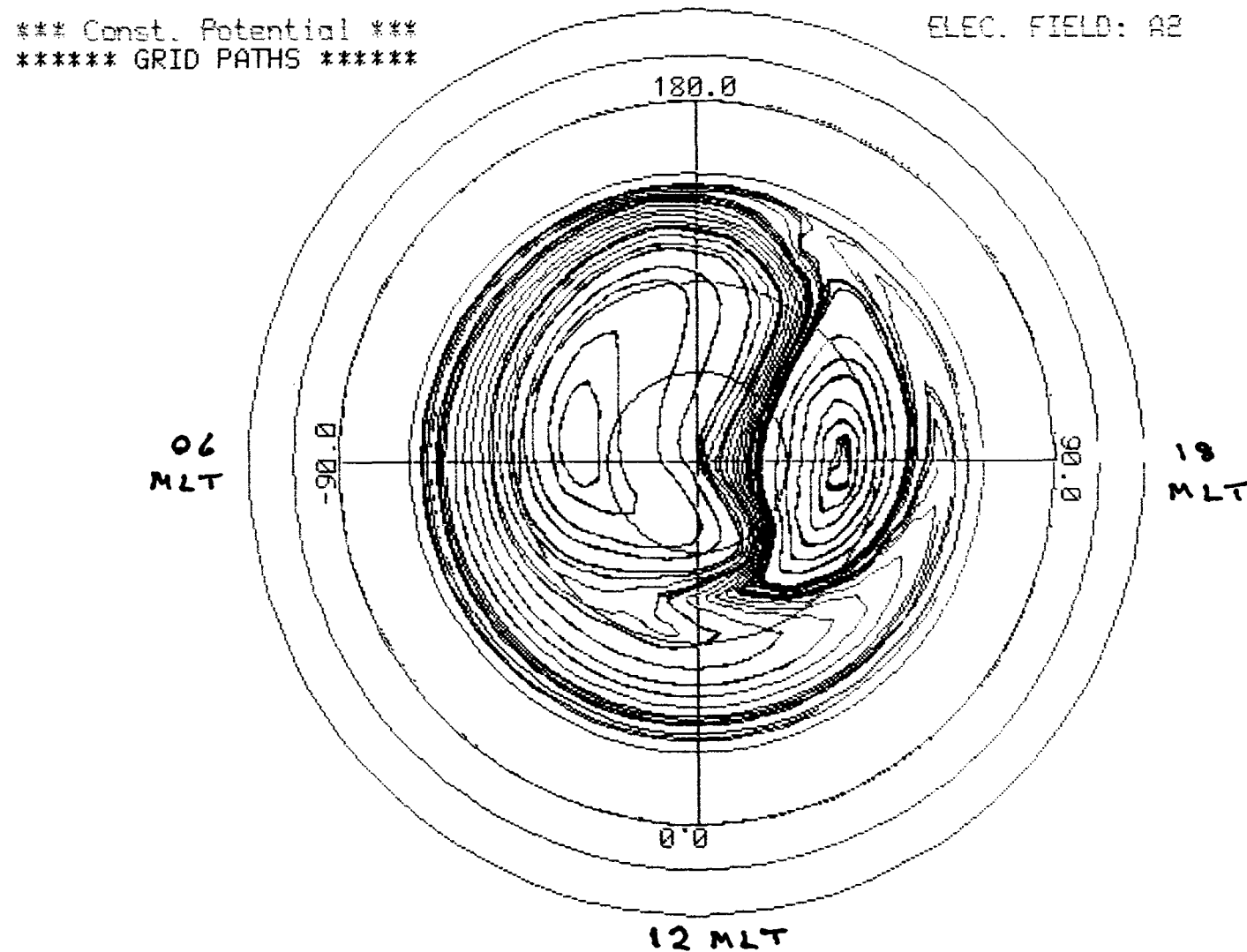


Figure 5. Convention paths traced by ionospheric flux tubes following the A2 polar electric field, as seen in solar and geomagnetic coordinates.

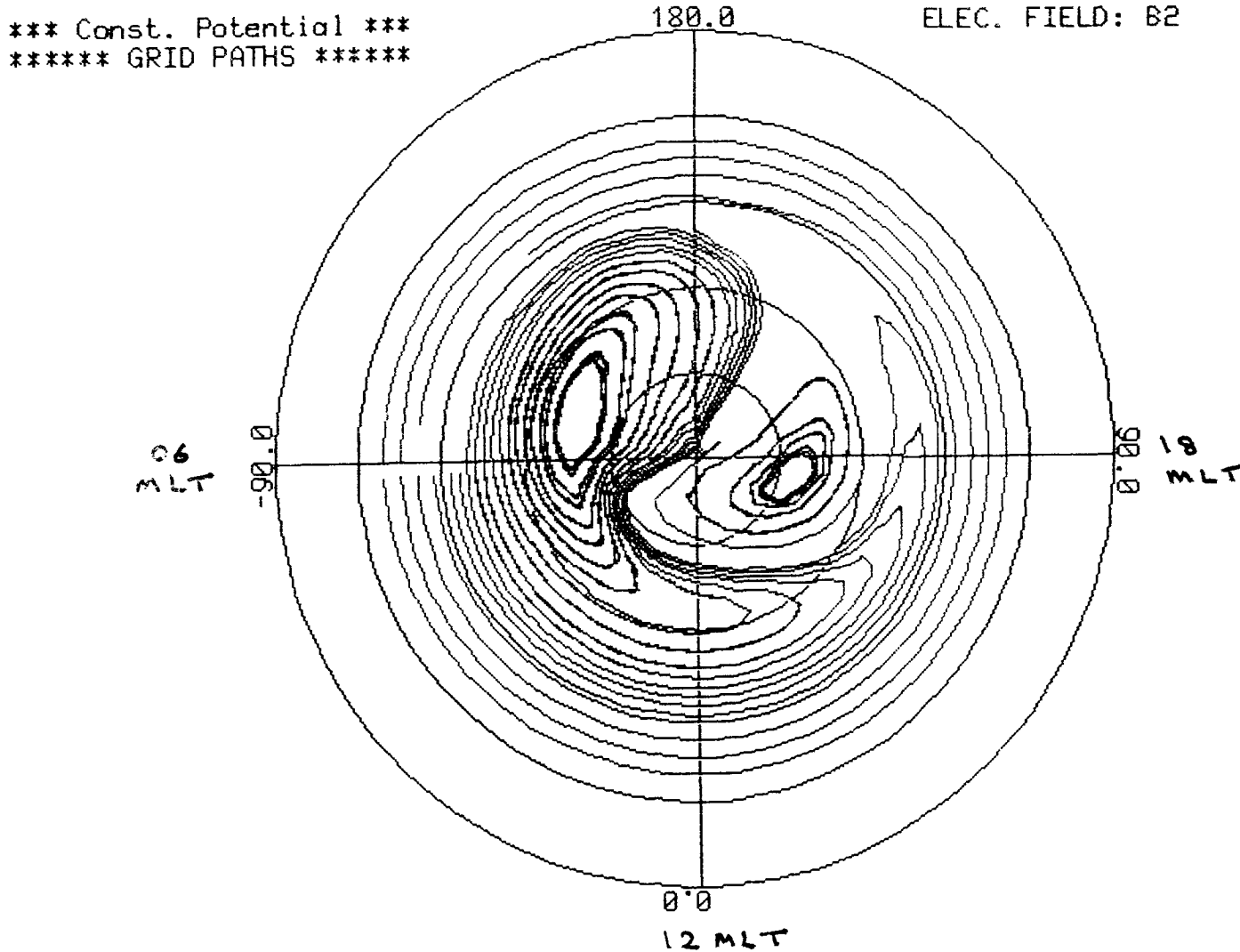
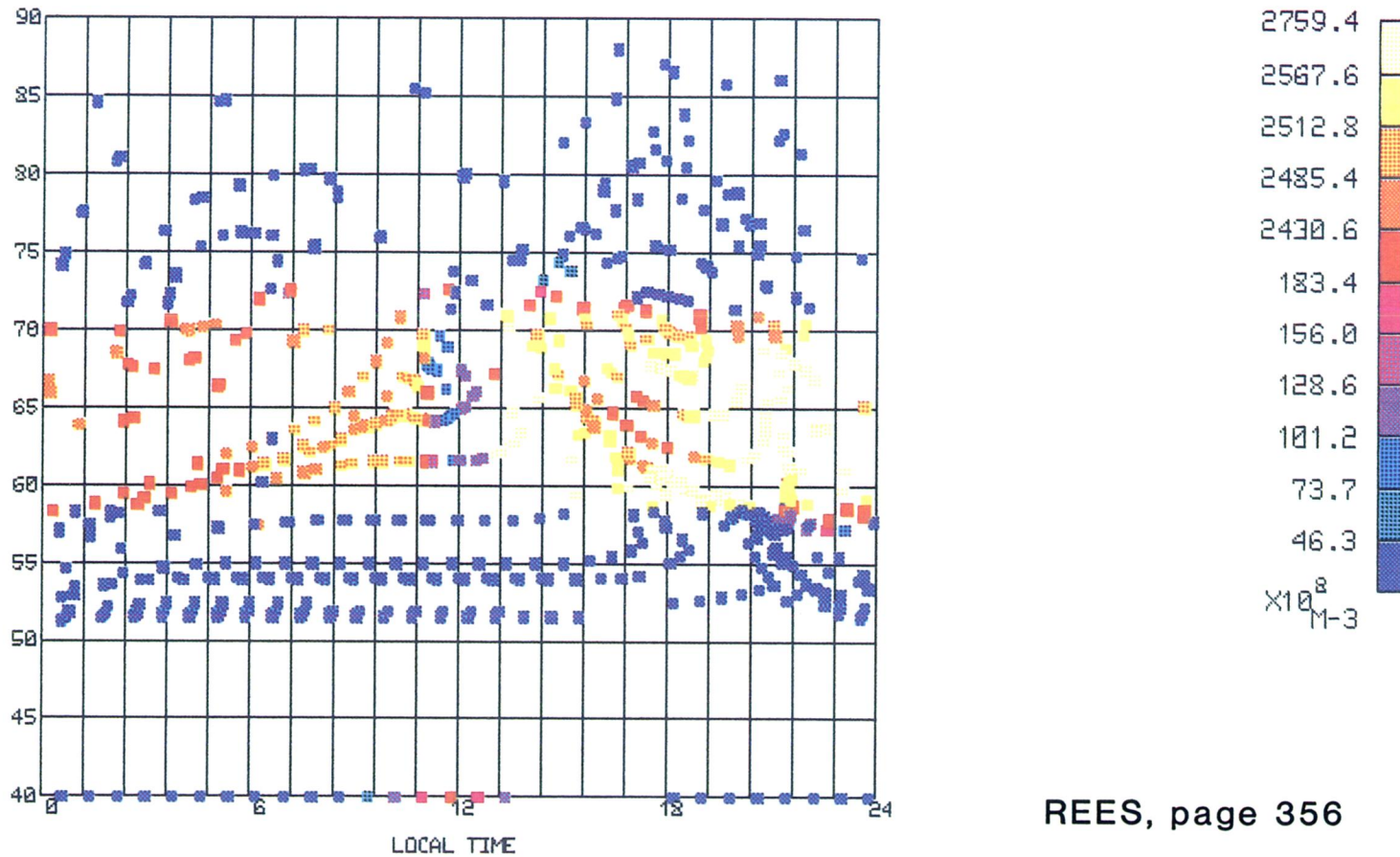


Figure 6. Convection paths traced by ionospheric flux tubes following the B2 polar electric field, as seen in solar and geomagnetic coordinates. The contrast between the concentration of paths over the dusk (A2) and dawn (B2) sides of the polar cap is the most striking feature.

HEIGHT: 160Km
UT: 0.00

*** ELECTRON DENSITY PLOT ***

DATA-FILE:D010000.ELD



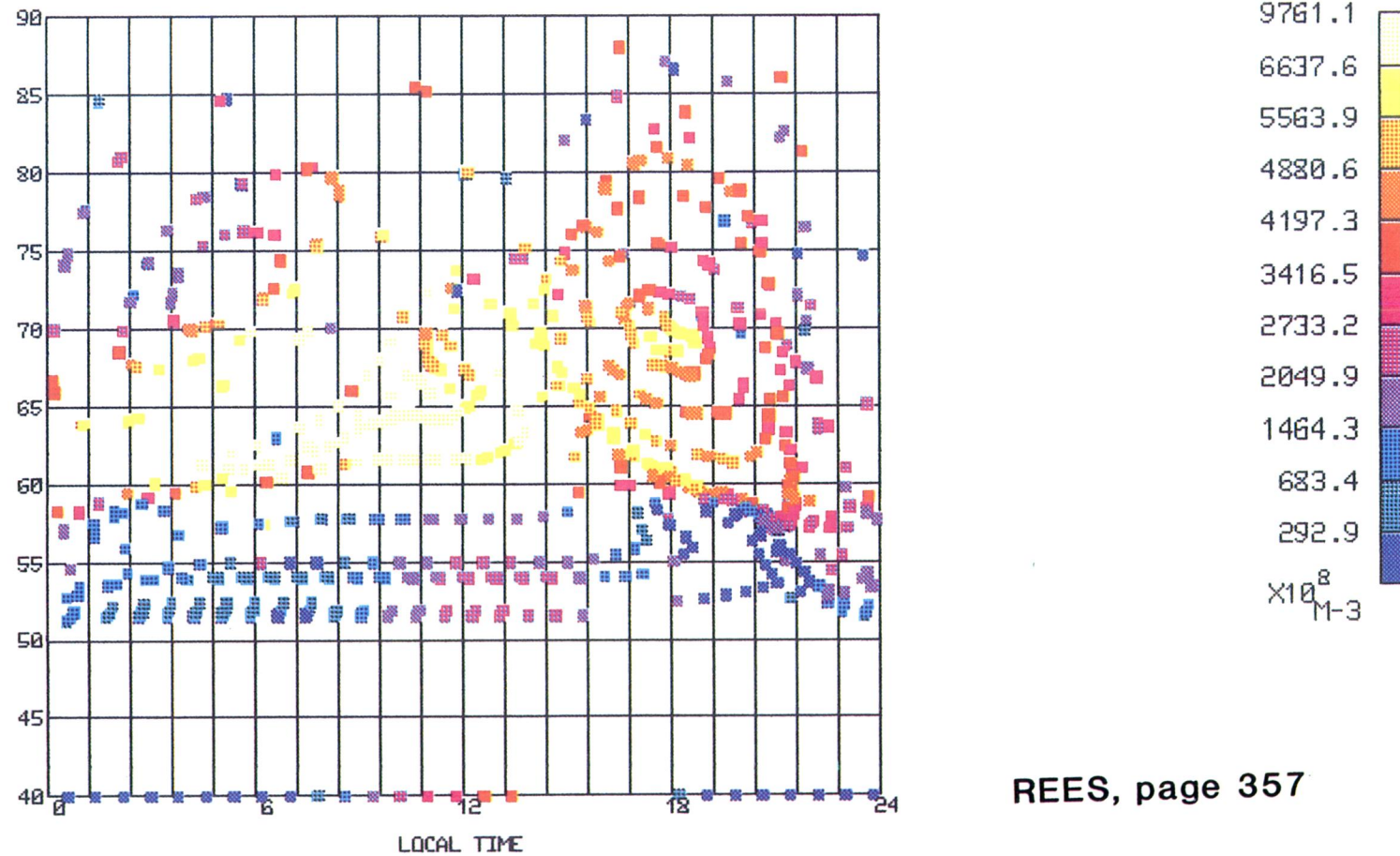
REES, page 356

Figure 7. Polar plasma densities at 160 km altitude produced by the winds and electric fields (convection) due to the A2 electric field and the same precipitation used in the original 'Sheffield' study. This study has been carried out for conditions of (northern) winter solstice, so that there is little solar photo-ionization within the auroral oval and polar cap regions. It can be seen that the plasma density enhancement is strictly limited to the vicinity of the auroral oval and its associated precipitation.

HEIGHT: 320Km
UT: 0.00

*** ELECTRON DENSITY PLOT ***

DATA-FILE:D010000.ELD



REES, page 357

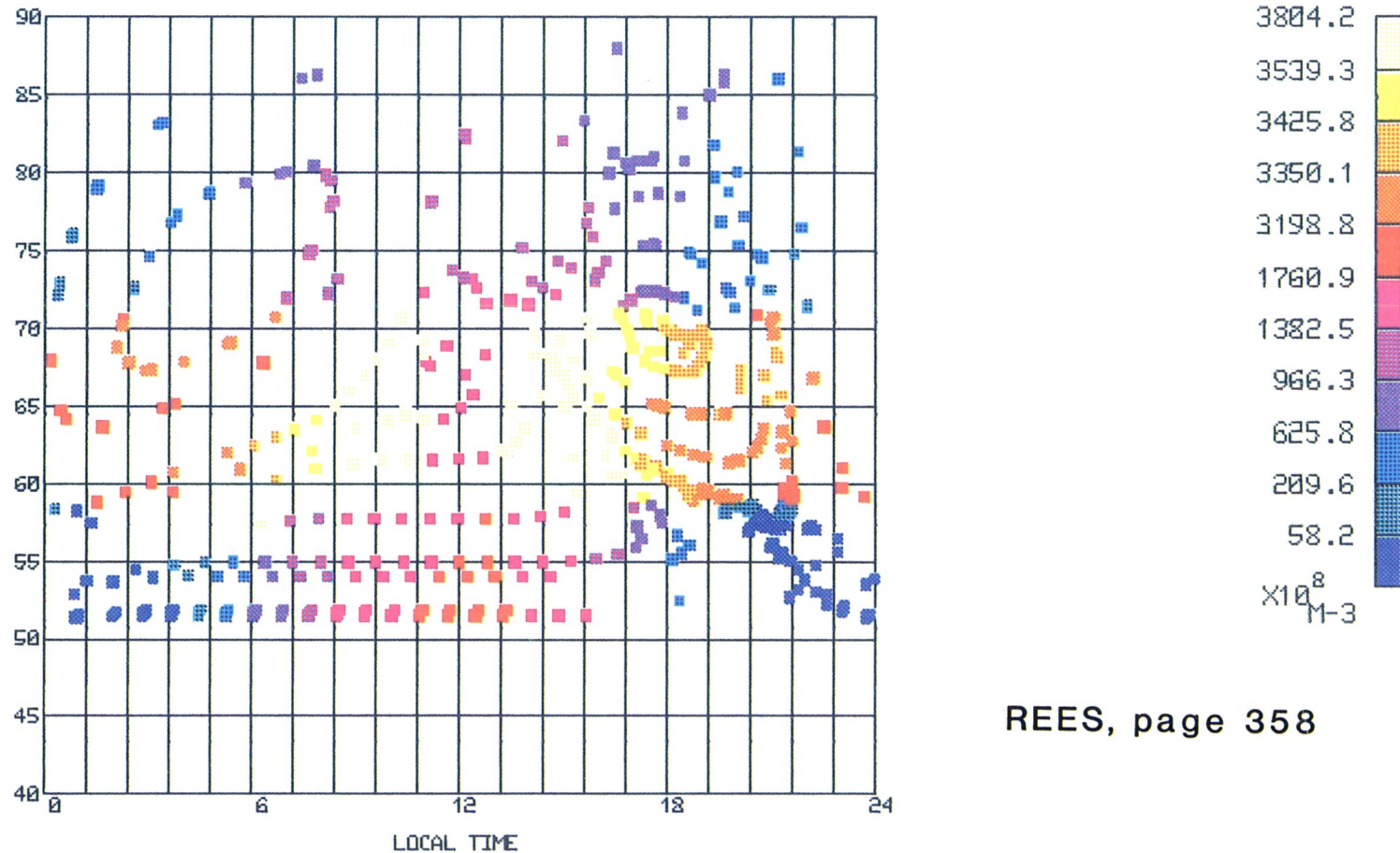
Figure 8. Same as Figure 7, but at 320 km. Transport effects are now very important, and there is an intense plume of ionisation carried anti-sunward over the polar cap, away from the polar cusp region, by the strong anti-sunward ion convection velocities in the dusk region of the polar cap.

HEIGHT: 160Km
UT: 0.00

*** ELECTRON DENSITY PLOT ***

DATA-FILE:D020000.ELD

358



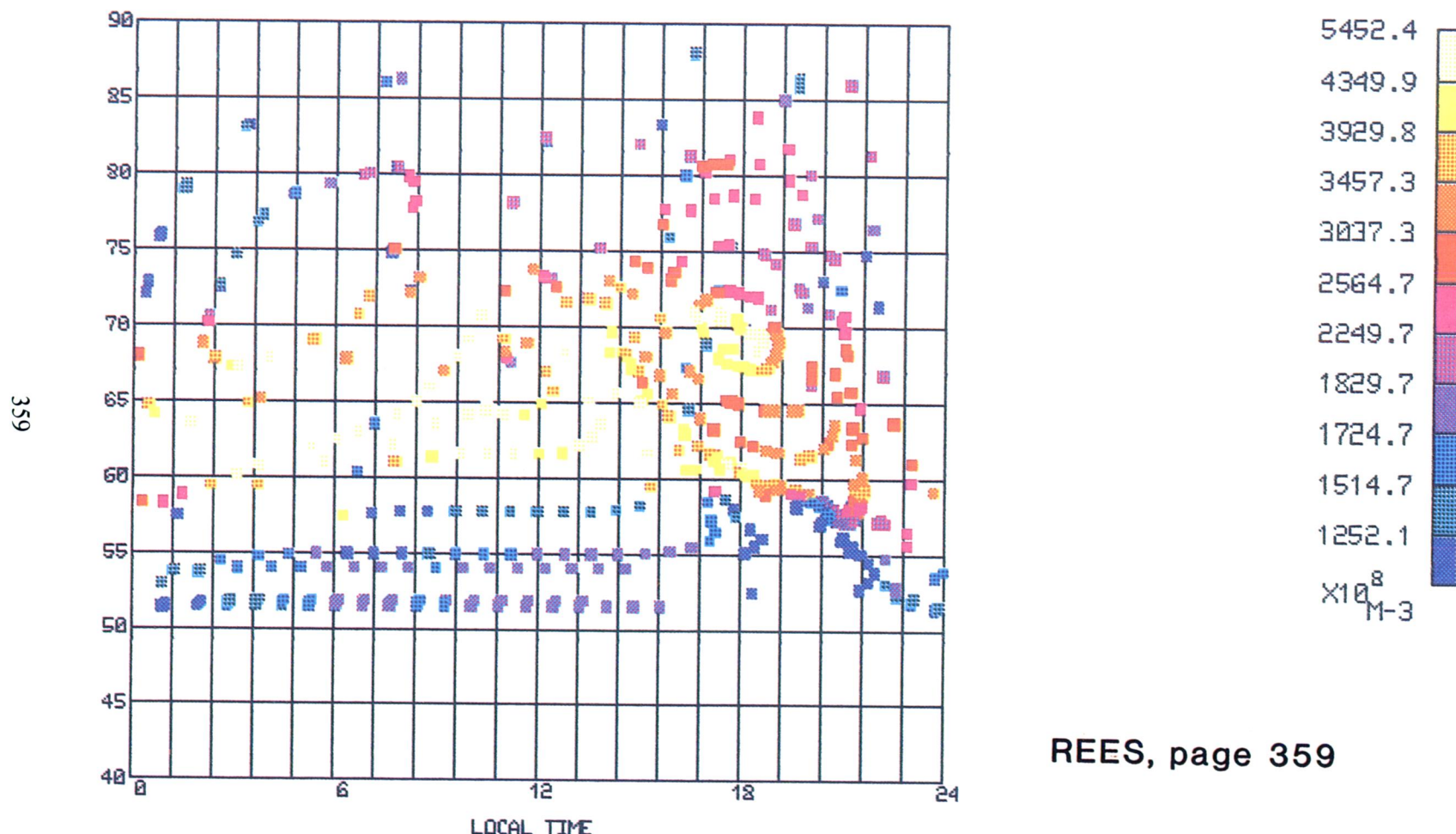
REES, page 358

Figure 9. Same as Figure 7, at 160 km altitude, but for (northern) summer solstice conditions. Despite the much higher solar photo-ionisation source, the actual electron densities, within the auroral oval, and on the dayside, at sub-auroral latitudes, are lower than those generated in the winter solstice model.

HEIGHT: 320Km
UT: 0.00

*** ELECTRON DENSITY PLOT ***

DATA-FILE:D020000.ELD



REES, page 359

Figure 10. Same as Figure 9, but at 320 km altitude.

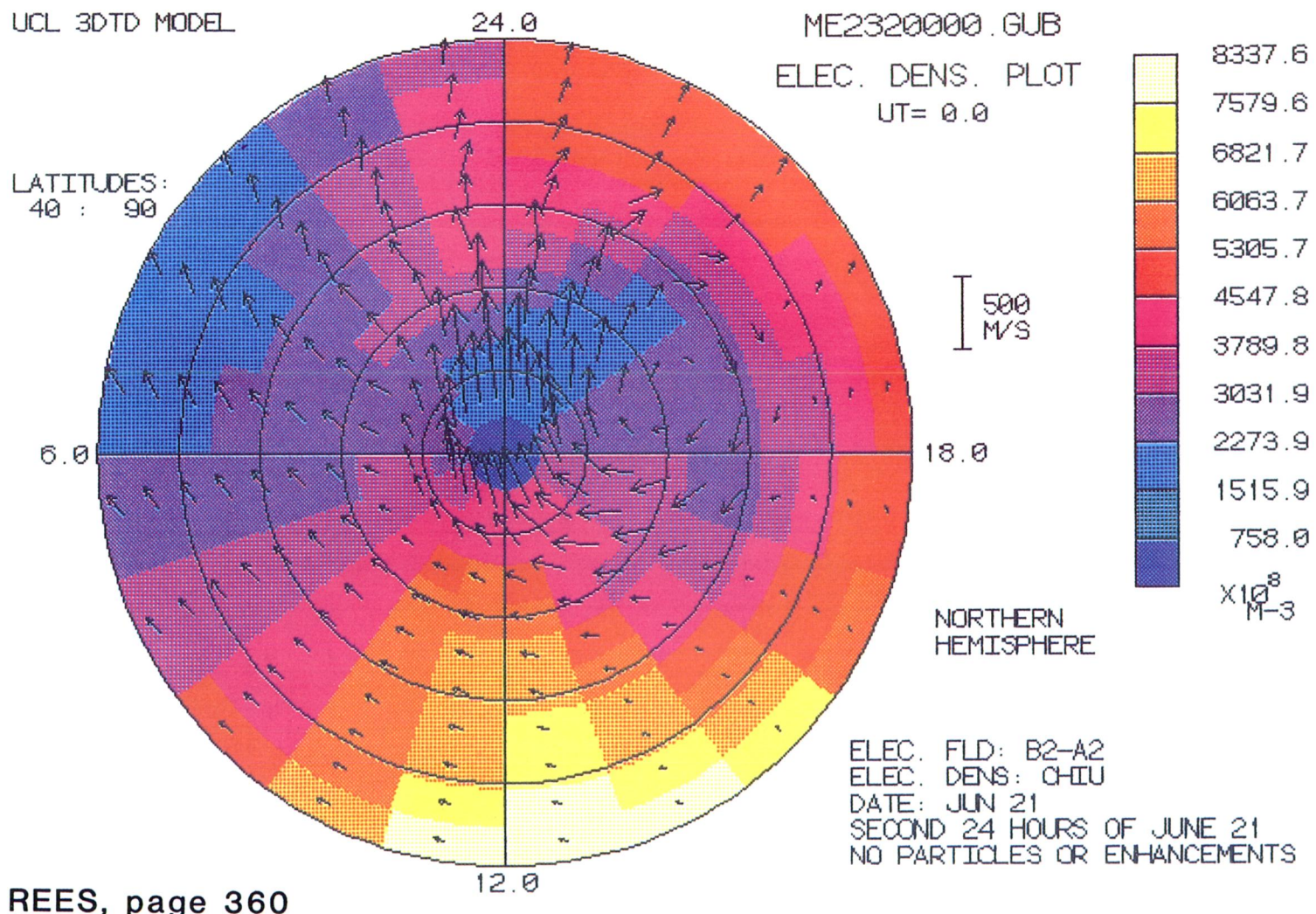


Figure 11. Thermospheric wind system at 320 km produced by the 'Chiu' global ionospheric model, with the same polar electric field as used to produce Figure 2, but for the June solstice. The electron densities are rather lower, at mid-latitudes than for the Dec. solstice.